A Novel Series of Efficient Thiophene-Based Light-Emitting Conjugated Polymers and Application in Polymer Light-Emitting Diodes

Jian Pei, Wang-Lin Yu, and Wei Huang*

Institute of Materials Research and Engineering, National University of Singapore, 3 Research Link, Singapore 117602, Republic of Singapore

Alan J. Heeger

Institute for Polymers and Organic Solids, University of California at Santa Barbara, Santa Barbara, California 93106-5090

Received August 20, 1999; Revised Manuscript Received January 19, 2000

ABSTRACT: A novel series of soluble conjugated polymers, poly[1,4-bis(4-alkyl-2-thienyl)-2,5-disubstituted phenylene]s, with different substituents on the phenylene ring (hydrogen, methyl group, or decyloxy group) and on the thiophene ring (*n*-hexyl chain or cyclohexyl group) were synthesized through $FeCl_3$-oxidative polymerization. The structures of the polymers were fully verified by FT−IR, ^1H and ^{13}C NMR, and element analysis. The high regioregularity of head-to-head linkage between two adjacent thiophene rings in the polymers was demonstrated. The electronic spectra of the polymers can be tuned by changing the substitution on both the phenylene and thiophene rings, emitting blue to green light. The electronic structures of the polymers can also be tuned by different substitutions, as demonstrated by electrochemical measurements (cyclic voltammetry). The absolute photoluminescence (PL) efficiencies of the polymers in neat films, which can be remarkably effected by the substitution on both the phenylene ring and the thiophene ring, can be up to 29%, much higher than the PL efficiencies in other polythiophene-based light-emitting materials. It was demonstrated that inserting substituted phenylene rings into the backbone of polythiophene is a useful approach to improve the PL efficiency of thiophene-based conjugated polymers. Blue to green electroluminescence (EL) was realized from some of the new polymers in single-layered light-emitting diodes with the configuration of ITO/polymer film/Ca or Al. One green light-emitting diode fabricated from the green-emissive polymer with the highest PL efficiency gave rise to the best EL performance, turning on at ∼8V and reaching an external EL quantum efficiency of 0.1%.

Introduction

Conjugated polymers have attracted considerable attention as a novel class of organic semiconductors in the past decade because of their promising electronic and optical applications.[1−6] In particular, following the discovery of electroluminescence (EL) in a conjugated polymer,[1] enormous efforts have been made toward the development of conjugated polymers as light-emitting materials,[7] which has generated a new promising display technology, polymer light-emitting diodes (PLEDs).[8,9] In the categories of conjugated polymers, polythiophene and derivatives occupy an important position. In the past two decades, extensive and intensive studies have been devoted to the synthetic methodologies, structural characterization, electrochemical properties, stability, electrical conductivity, and a variety of applications of processable polythiophene derivatives (PTs).[10−12] For the application as active materials in PLEDs, the most attractive characters of PTs are their good stability both in neutral state and in doped states and their wide electronic and optical tunability. By attaching different functional groups and controlling regioregularity and steric interaction, light emission ranging from blue to near-infrared spectra has been demonstrated in PTs.[13,14]

One of the most important considerations in developing conjugated polymers for PLEDs is the photoluminescence (PL) quantum efficiency (η_{PL}) of the polymers, which associates with the electroluminescence (EL) quantum efficiency (η_{EL}) by a theoretical relation of $\eta_{EL} \leq {}^1/_4\eta_{PL}$.[15] Unfortunately, PTs exhibit very low PL quantum efficiency, typically 1−3%, in solid films. The low PL quantum efficiency limits the application of PTs in PLEDs. Some studies on PL processes in oligo- and polythiophenes attribute the low PL efficiency to the intersystem crossing of excitons to triplet states.[16,17] Suppressing the three-dimensional (3-D) diffusion of excitons and confining excitons to 1-D diffusion should enhance the PL efficiency. This has been proven by the improvement of PL efficiency through dispersing polythiophenes into liquid solutions or solid solutions.[16,18] From the point of view of molecular engineering, recently a 2,5-dioctyl-phenylene group was introduced into polythiophene on the 3-position of every thiophene ring to enhance the separation between conjugated main chains. This molecular modification increases the PL efficiency to a level of 24%.[16,19] On the other hand, the intrinsic features of the electronic structure of polythiophene backbone should also be responsible for the low PL efficiency of PTs. In fact, most of other conjugated polymers, especially those based on six-member aromatic rings, such as poly(*p*-phenylenevinylene) and derivatives (PPVs),[20] substituted poly(*p*-phenylenes) (PPPs),[21] and substituted polyfluorenes (PFs),[22,23] generally have much higher PL efficiencies than PTs. Most recently, Gigli et al. reported a significant increase of PL efficiency in thiophene oligomers by modifying the backbone structure.[24] In their approach, the central thienyl in a pentamer of thiophene was functionalized by bonding two oxygen atoms to the sulfur atom. The

* To whom all correspondence should be addressed. Telephone: (65) 874 8592/8593. Fax: (65) 874 8592. E-mail: wei-huang@imre.org.sg.

10.1021/ma9914220 CCC: $19.00
Published on Web 03/04/2000

Chart 1

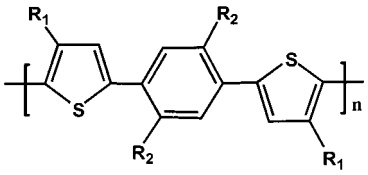

modification increased the PL efficiency from 2−3% to 11−13%. Further functionalization with methyl substituents on the other four "lateral" thienyls in a head-to-head pattern led the PL efficiency up to 37 ± 3%. This demonstrates the possibility of improving the PL efficiency of thiophene-based oligomers and polymers by backbone modifications.

In this contribution, we present a new approach, based on inserting a phenylene ring into the backbone of polythiophene, in an effort to developing highly efficient thiophene-based light-emitting polymers. The basic structure of the polymers is illustrated in Chart 1. From appropriate starting monomers, the polymers can be synthesized using the same chemical polymerization methods as those in the synthesis of conventional PTs, including oxidative polymerization and cross-coupling reaction. The polymers obtained by $FeCl_3$-oxidative polymerization are reported in this contribution. Reynolds et al. even reported similar backbone structure in their electrically conductive polymers;[25] however, the optical properties were not thoroughly studied, and there were no substituents on the thiophene rings in their structures. The substituents on the thiophene rings not only enable good solubility of the resulting polymers, which is essential for light-emitting polymers, and provide the opportunity of tuning the electronic and optical properties of the resulting polymers but also allow us to control the connection manner between two adjacent thiophene rings as a defined head-to-head pattern. The head-to-head conformation makes the polymer chains highly twisted. As demonstrated in poly(3-alkylthiophene)s, the high twist of polymer chains caused by the head-to-head conformation may significantly increase PL quantum efficiency in comparison with the head-to-tail conformation.[26]

Experimental Section

Materials. Ether and tetrahydrofuran (THF) were dried and distilled under argon from metal sodium powder and benzophenone. Chloroform was purified by distillation with calcium hydride. All chemicals were purchased from the Aldrich Chemical Co. and used as received unless otherwise stated.

Characterization. The gel permeation chromatography (GPC) measurements were performed on a Perkin-Elmer model 200 HPLC system at room temperature using THF (HPLC grade) as the eluent. The molecular weights and the molecular weight distributions were calculated on the basis of monodispersed polystyrene standards. ^{1}H (300 MHz) and ^{13}C (75.5 MHz) NMR spectra were collected on a Bruker AMX300 spectrometer. Chemical shifts (δ) were reported in ppm downfield from tetramethylsilane (TMS). UV−vis spectra were recorded on a Shimadzu 3101 spectrometer. Infrared spectra measurements were made in KBr pressed pellets on a Bio-Rad FTS 165 FT−IR spectrometer. Fluorescence measurements were carried out on a Perkin-Elmer LS 50B photoluminescent spectrometer with a xenon lamp as light source. Thermogravimetric analysis (TGA) of polymer powders were conducted on a Du Pont Thermal Analyst 2100 system with a TGA 2950 thermogravimetric analyzer. A heating rate of 20 °C/min with an air and nitrogen flow of 75 cm^3/min was used with the runs being conducted from room temperature to 1000 °C. Cyclic voltammetry was carried out with a BAS 100 Electrochemical analyzer at a potential scan rate of 40 mV/s. In each case, a glassy carbon disk electrode (0.2 cm^2) coated with a thin polymer film, drop-cast from the polymer solution in THF, was used as working electrode. A platinum wire was used as counter electrode and a silver wire was used as a quasi-reference electrode. The anodic and cathodic scans were performed separately using new films for each sample. All of the potential values quoted in this paper are referred to the Ag quasi-reference electrode, which has the electrochemical potential of −0.02 V versus SCE. All of the electrochemical experiments were performed in a glovebox under argon atmosphere at room temperature.

1. Monomer Syntheses. 3-Hexylthiophene and 3-cyclohexylthiophene were prepared from 3-bromothiophene following the literature procedure.[14,27]

1,4-Dibromo-2,5-didecyloxybenzene. A solution of bromine (50 mmol) in 40 mL of carbon tetrachloride was slowly added to a solution of 1,4-didecyloxybenzene (20 mmol), which was prepared form hydroquinone and 1-bromodecane,[28] in 100 mL of carbon tetrachloride in a period of 2 h. The mixture was stirred for 1 day at room temperature. After working up, the residue was recrystallized with ethanol to give white crystals (yield: 85%). ^{1}H NMR ($CDCl_3$, 300 MHz, ppm): δ 7.09 (2H, s, Ar−H), 3.92−3.98 (4H, t, J = 6.6 Hz, OCH_2), 1.86−1.94 (4H, m, CH_2), 1.48−1.55 (4H, m, CH_2), 1.30−1.37 (24H, m, CH_2), 0.87−0.91 (6H, t, J = 6.8 Hz, CH_3).

1,4-Bis(4-hexyl-2-thienyl)-2,5-dimethylbenzene (**2a**). *n*-Butyllithium (18.8 mL, 1.6 M solution in hexane, 30 mmol) was added dropwise to a solution of diisopropylamine (3.04 g, 30 mmol) in 50 mL of dry THF at 0 °C. After it was stirred for 0.5 h at 0 °C, the mixture was cooled to −78 °C. A solution of 3-hexylthiophene (5.04 g, 30 mmol) in 20 mL of dry THF was added through a syringe under nitrogen atmosphere. The mixture was stirred for 2 h at this temperature and transferred to a solution of anhydrous zinc chloride (4.36 g, 32 mmol) in 15 mL of dry THF via a double-tipped plastic needle. The mixture was stirred for 1 h at −78 °C and allowed to warm to room temperature for an additional hour. The mixture was transferred dropwise to a solution of *p*-dibromoxylene (3.17 g, 12 mmol) and $Pd(PPh_3)_4$ (140 mg, 0.12 mmol) in 10 mL of dry THF. The resulting reaction mixture was stirred for 10 h at room temperature, refluxed for 10 h, and then was quenched by being poured into a saturated solution of ammonium chloride. The aqueous layer was extracted three times with hexane. The combined organic layers were washed with water and brine and dried over magnesium sulfate. The solvent was removed by vacuum evaporation, and the residue was purified by recrystallization or flash chromatography (silica gel, hexane as eluent) to give white needle crystals (4.68 g, yield: 89%). Anal. Calcd for $C_{28}H_{38}S_2$: C, 76.66, H, 8.73, S, 14.61. Found: C, 75.98, H, 8.04, S, 14.65. FT−IR (λ, cm^{-1}): 2950, 2920, 2851, 1502, 1468, 1188, 869, 841, 728. ^{1}H NMR ($CDCl_3$, 300 MHz, ppm): 7.31 (2H, s, Ar−H), 6.93 (4H, s, Th−H), 2.61−2.66 (4H, t, J = 7.4 Hz, CH_2), 2.43 (6H, s, Ar−CH_3), 1.61−1.71 (4H, m, CH_2), 1.27−1.43 (12H, m, CH_3), 0.88−0.92 (6H, m, CH_3). ^{13}C NMR ($CDCl_3$, 75.5 MHz, ppm): 143.36, 142.31, 133.60, 133.04, 132.38, 127.75, 119.60, 31.59, 30.49, 30.35, 28.92, 22.50, 20.51, 13.96. EI MS (*m*/*e*): 438 (100%).

1,4-Bis(4-hexyl-2-thienyl)benzene (**2b**). **2b** was obtained from 3-hexylthiophene and 1,4-dibromobenzene following a procedure similar to that described for **2a** (yield: 89%). Anal. Calcd for $C_{26}H_{34}S_2$: C, 76.04; H, 8.34; S, 15.61. Found: C, 76.04; H, 8.96; S, 16.53. FT−IR (λ, cm^{-1}): 2955, 2926, 2850, 1508, 1458, 823. ^{1}H NMR ($CDCl_3$, 300 MHz, ppm): 7.58 (1H, s, Ar−H), 7.17−7.18 (1H, d, J = 1.1 Hz, Th−H), 6.87−6.88 (1H, d, J = 1.1 Hz, Th−H), 2.60−2.65 (4H, t, J = 7.5 Hz, CH_2), 1.61−1.71 (4H, m, CH_2), 1.26−1.52 (12H, m, CH_2), 0.88−0.93 (6H, t, J = 6.8 Hz, CH_3). ^{13}C NMR ($CDCl_3$, 75.5 MHz, ppm): 144.29, 143.39, 133.48, 125.87, 124.34, 119.41, 31.60, 30.54, 30.33, 28.92, 22.51, 13.99. EI MS (*m*/*e*): 410 (100%).

1,4-Bis(4-hexyl-2-thienyl)-2,5-didecyloxybenzene (**2c**). **2c** was obtained from 3-hexylthiophene and 1,4-dibromo-2,5-didecyloxybenzene following a procedure similar to that de-

scribed for **2a** (yield: 83%). Anal. Calcd for $C_{46}H_{74}S_2O_2$: C, 76.40, H, 10.31, S, 8.87. Found: C, 75.71, H, 9.81, S, 8.98. FT−IR (λ, cm^{-1}): 2920, 2851, 1506, 1472, 1200, 1182, 1020, 991, 947, 858, 841, 721, 700, 590. ^1H NMR ($CDCl_3$, 300 MHz, ppm): 7.37 (2H, s, Ar−H), 7.20 (2H, s, Th−H), 6.91 (2H, s, Th−H), 4.04−4.09 (4H, t, J = 6.45 Hz, OCH_2), 2.60−2.65 (4H, t, J = 7.5 Hz), 1.86−1.91 (4H, m, CH_2), 1.63−1.66 (4H, m, CH_2), 1.54−1.55 (6H, m, CH_2), 1.27−1.33 (28H, m, CH_2), 0.86−0.90 (12H, m, CH_3). ^{13}C NMR ($CDCl_3$, 75.5 MHz, ppm): 149.60, 138.71, 126.60, 125.71, 125.26, 123.12, 111.27, 70.29, 31.72, 29.23, 29.19, 29.15, 29.10, 26.05, 25.91, 22.57, 14.02. EI MS (*m*/*e*): 722 (100%).

1,4-Bis(4-cyclohexyl-2-thienyl)-2,5-dimethylbenzene (**2d**). **2d** was obtained from 3-cyclohexylthiophene and 2,5-dibromo-*p*-xylene following a procedure similar to that described for **2a** (yield: 84%). Anal. Calcd for $C_{28}H_{34}S_2$: C, 77.37; H, 7.88; S, 14.75. Found: C, 77.19; H, 7.87; S, 15.16. FT−IR (λ, cm^{-1}): 2934, 2851, 1506, 1489, 1387, 1263, 1190, 1055, 961, 932, 889, 872, 835, 814, 754, 741, 704. ^1H NMR ($CDCl_3$, 300 MHz, ppm): 7.33 (2H, s, Ar−H), 6.99 (2H, s, Th−H), 6.94 (2H, s, Th−H), 2.50−2.70 (2H, m, CH), 2.44 (6H, s, CH_3), 1.92−2.08 (4H, m, CH_2), 1.64−1.90 (6H, m, CH_2), 1.22−1.44 (10H, m, CH_2). ^{13}C NMR ($CDCl_3$, 75.5 MHz, ppm): 149.14, 142.22, 133.68, 133.06, 132.48, 126.66, 118.14, 39.72, 34.12, 26.59, 26.16, 20.66. EI MS (*m*/*e*): 434 (100%).

1,4-Bis(4-cyclohexyl-2-thienyl)benzene (**2e**). **2e** was obtained from 3-cyclohexylthiophene and 1,4-dibromobenzene following a procedure similar to that described for **2a** (yield: 86%). Anal. Calcd for $C_{26}H_{30}S_2$: C, 76.80; H, 7.45; S, 15.75. Found: C, 76.82; H, 7.20; S, 16.00. FT−IR (λ, cm^{-1}): 2934, 2853, 1506, 1472, 1196, 1111, 1020, 893, 870, 845, 824, 743, 712, 610. ^1H NMR ($CDCl_3$, 300 MHz, ppm): 7.57 (4H, s, Ar−H), 7.22 (2H, d, J = 1.4 Hz, Th−H), 6.87−6.88 (2H, t, J = 1.0 Hz, Th−H), 2.55−2.63 (2H, m, CH), 1.22−2.02 (20H, m, CH_2). ^{13}C NMR ($CDCl_3$, 75.5 MHz, ppm): 150.03, 143.20, 133.53, 125.86, 123.11, 117.93, 39.73, 34.02, 26.48, 26.05. EI MS (*m*/*e*): 406 (100%).

1,4-Bis(4-cyclohexyl-2-thienyl)-2,5-didecyloxybenzene (**2f**). **2f** was obtained from 3-cyclohexylthiophene and 1,4-dibromo-2,5-didecyloxybenzene following a procedure similar to that described for **2a** (yield: 84%). Anal. Calcd for $C_{46}H_{70}S_2O_2$: C, 76.82; H, 9.81; S, 8.92. Found: C, 76.36; H, 10.48; S, 9.65. FT−IR (λ, cm^{-1}): 2922, 2851, 1506, 1472, 1192, 1067, 1024, 947, 870, 839, 758, 655. ^1H NMR ($CDCl_3$, 300 MHz, ppm): 7.44 (2H, d, J = 1.3 Hz, Th−H), 7.19 (2H, s, Ar−H), 6.92 (2H, s, Th−H), 2.56−2.64 (2H, m, CH), 1.22−2.02 (52H, m, CH_2), 0.87−0.90 (6H, t, J = 8.5 Hz, CH_3). ^{13}C NMR ($CDCl_3$, 75.5 MHz, ppm): 149.27, 148.78, 138.81, 125.61, 122.97, 118.73, 112.65, 69.62, 39.76, 34.18, 31.91, 29.60, 29.53, 26.53, 26.41, 26.19, 22.68, 14.12. EI MS (*m*/*e*): 718 (100%).

2. Polymer Syntheses. Poly[1,4-bis(4-hexyl-2-thienyl)-2,5-dimethyl phenylene] (Polymer **3a**). A solution of anhydrous ferric chloride (9 mmol) in 100 mL of dry chloroform was added dropwise to a stirred solution of **2a** (3 mmol) in 40 mL of dry chloroform at 0 °C. The mixture was stirred for 24 h at 0 °C with a slowly dynamic flow of nitrogen. The blue-black solution was poured into stirred methanol (500 mL) to generate plenty of blue-green precipitate. The solid was collected by filtration and washed with methanol and water. The residue was dissolved in THF and dedoped by stirring in concentrated aqueous ammonium hydroxide (or 50% aqueous hydrazine) overnight. The yellow solid was isolated by filtration and washed with methanol and water again. After being dried, the solid was washed with acetone and then extracted with chloroform in Soxhlet. After the chloroform was removed by vacuum evaporation, a light yellow solid was obtained (yield: 83%). Anal. Calcd for $C_{28}H_{36}S_2$: C, 77.01; H, 8.31; S, 14.68. Found: C, 76.44; H, 8.82; S, 14.95. FT−IR (λ, cm^{-1}): 2954, 2922, 2856, 1497, 1451, 1374, 1254, 1181, 1107, 1018, 876, 849, 718. ^1H NMR ($CDCl_3$, 300 MHz, ppm): 7.38 (2H, s, Ar−H), 6.99 (2H, s, Th−H), 2.60−2.70 (4H, b, CH_2), 2.17 (6H, s, Ar−CH_3), 1.52−1.65 (4H, b, CH_2), 1.23−1.36 (12H, b, CH_2), 0.82−0.96 (6H, b, CH_3). ^{13}C NMR ($CDCl_3$, 75.5 MHz, ppm): 142.39, 141.50, 133.32, 133.14, 132.428, 128.63, 128.17, 31.71, 30.83, 30.64, 29.18, 22.82, 20.87, 14.13.

Poly[1,4-bis(4-hexyl-2-thienyl)phenylene] (Polymer **3b**). **2b** was polymerized according to the procedure described for polymer **3a** (yield: 78%). Anal. Calcd for $C_{26}H_{32}S_2$: C, 76.41; H, 7.89; S, 15.69. Found: C, 76.42; H, 8.20; S, 16.76. FT−IR (λ, cm^{-1}): 2955, 2923, 2853, 1507, 1466, 1437, 1378, 1212, 1031, 843, 721. ^1H NMR ($CDCl_3$, 300 MHz, ppm): 7.62 (4H, s, Ar−H), 7.25 (2H, s, Th−H), 2.40−2.66 (4H, b, CH_2), 1.55−1.68 (4H, b, CH_2), 1.15−1.55 (12H, b, CH_2), 0.78−0.96 (6H, b, CH_3). ^{13}C NMR ($CDCl_3$, 75.5 MHz, ppm): 143.52, 143.13, 133.24, 128.27, 125.91, 124.66, 31.58, 30.63, 29.07, 28.94, 22.50, 13.91.

Poly[1,4-bis(4-hexyl-2-thienyl)-2,5-didecyloxyphenylene] (Polymer **3c**). **2c** was polymerized by 4 equiv of ferric chloride according to the procedure described for polymer **3a** (yield: 81%). Anal. Calcd for $C_{46}H_{72}S_2O_2$: C, 76.60; H, 10.06; S, 8.89. Found: C, 75.71; H, 9.81; S, 8.98. FT−IR (λ, cm^{-1}): 2956, 2921, 2851, 1507, 1437, 1375, 1210, 819, 723. ^1H NMR ($CDCl_3$, 300 MHz, ppm): 7.47 (1H, s, Ar−H), 7.25 (1H, s, Th−H), 4.10−4.12 (4H, t, OCH_2), 2.60−2.64 (4H, b, CH_2), 1.84−1.96 (4H, b, CH_2), 1.51−1.68 (10H, b, CH_2), 1.12−1.46 (28H, b, CH_2), 0.82−0.88 (12H, b, CH_3). ^{13}C NMR ($CDCl_3$, 75.5 MHz, ppm) 149.33, 141.85, 138.56, 129.29, 126.97, 122.67, 112.10, 69.61, 31.80, 31.67, 30.80, 29.52, 29.40, 29.16, 29.04, 26.25, 13.98.

Poly[1,4-bis(4-cyclohexyl-2-thienyl)-2,5-dimethyl phenylene] (Polymer **3d**). **2d** was polymerized according to the procedure described for polymer **3a** (yield: 73%). Anal. Calcd for $C_{28}H_{32}S_2$: C, 77.72; H, 7.46; S, 14.82. Found: C, 77.39; H, 7.30; S, 14.91. FT−IR (λ, cm^{-1}): 2924, 2849, 1490, 1387, 1263, 1184, 1124, 1020, 964, 889, 827, 818. ^1H NMR ($CDCl_3$, 300 MHz, ppm): 7.42 (2H, s, Ar−H), 7.07 (2H, s, Th−H), 2.69−2.77 (2H, m, CH), 2.54 (6H, s, CH_3), 1.21−1.98 (20H, b, CH_2). ^{13}C NMR ($CDCl_3$, 75.5 MHz, ppm): 148.69, 143.47, 134.21, 133.92, 133.30, 129.16, 128.38, 39.23, 37.36, 35.37, 27.48, 21.77.

Poly[1,4-bis(4-cyclohexyl-2-thienyl)phenylene] (Polymer **3e**). **2e** was polymerized according to the procedure described for polymer **3a** (yield: 76%). Anal. Calcd for $C_{26}H_{28}S_2$: C, 77.18; H, 6.98; S, 15.84. Found: C, 76.81; H, 7.95; S, 15.71. FT−IR (λ, cm^{-1}): 2924, 2851, 1449, 1198, 1111, 978, 891, 822. ^1H NMR ($CDCl_3$, 300 MHz, ppm): 7.65 (4H, s, Ar−H), 7.31 (2H, s, Th−H), 2.56−2.72 (2H, b, CH), 1.18−2.05 (20H, b, CH_2). ^{13}C NMR ($CDCl_3$, 75.5 MHz, ppm): 149.33. 143.82, 133.53, 127.43, 126.05, 122.80, 38.62, 34.66, 26.79, 26.28.

Poly[1,4-bis(4-cyclohexyl-2-thienyl)-2,5-didecyloxyphenylene] (Polymer **3f**). **2f** was polymerized with 4 equiv of ferric chloride according to the procedure described for polymer **3a** (yield: 84%). Anal. Calcd for $C_{46}H_{68}S_2O_2$: C, 77.04; H, 9.56; S, 8.94. Found: C, 76.67; H, 10.55; S, 9.84. FT−IR (λ, cm^{-1}): 2932, 2851, 1420, 1387, 1227, 1190, 1020, 988, 964, 889, 844, 721. ^1H NMR ($CDCl_3$, 300 MHz, ppm): 7.64 (4H, s, Ar−H), 7.32 (2H, s, Th−H), 2.55−2.70 (2H, b, CH), 1.21−2.05 (20H, b, CH_2). ^{13}C NMR ($CDCl_3$, 75.5 MHz, ppm): 149.07. 143.58, 133.31, 127.20, 125.92, 122.51, 38.37, 34.38, 29.64, 26.52.

3. Device Fabrication. Typical single-layered polymer light-emitting diodes were fabricated using these new polymers as the active materials. Indium−tin oxide (ITO)-coated glass (∼20 Ω/□) was used as the substrate. Polymer films were spin-cast on the substrates from their solutions in 1,1,2,2-tetrachloroethane. The thickness of the films was around 100 nm. A calcium or aluminum layer (100−200 nm) was then deposited on the top of the polymer films under the pressures around 10^{-6} Torr at the evaporating rates of 5−8 Å/s. Diode area was 15 mm^2 defined by the cathode. Device characteristics were measured with a calibrated Si photodiode. All of the processes and measurements were carried out inside a drybox filled with nitrogen. In forward bias, the ITO electrode was wired as the anode.

Results and Discussion

Preparation and Characterization. The general synthetic route toward the monomers of 2,5-disubstituted and unsubstituted 1,4-bis(4-alkyl-2-thienyl)benzenes and polymers is outlined in Scheme 1. 3-Substituted thiophenes were synthesized from 3-bromo-

Scheme 1. Synthetic Route

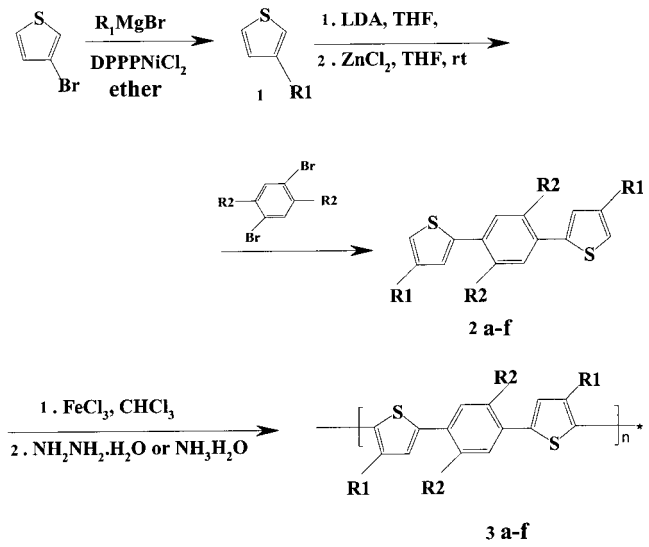

a: R_1 = hexyl, R_2 = methyl. b: R_1 = hexyl, R_2 = H.

c: R_1 = hexyl, R_2 = decyloxy. d: R_1 = cyclohexyl, R_2 = methyl.

e: R_1 = cyclohexyl, R_2 = H. f: R_1 = cyclohexyl, R_2 = decyloxy.

Table 1. ^{1}H NMR Chemical Shifts and Assignment of Monomers 2a−f and Polymers 3a−f

compound	H-1	H-7	H-5	compound	H-1	H-7	H-5
2a	7.31	6.93	6.93	**2d**	7.33	6.99	6.94
3a	7.38		6.99	**3d**	7.42		7.07
2b	7.58	7.18	6.88	**2e**	7.57	7.22	6.88
3b	7.62		7.25	**3e**	7.65		7.31
2c	7.20	7.37	6.91	**2f**	7.19	7.44	6.92
3c	7.25		7.45	**3f**	7.26		7.64

thiophene through the Grignard coupling reaction with hexylmagnesium bromide or cyclohexylmagnesium bromide catalyzed by [1,3-bis(diphenylphosphino)propane]-dichloronickel(II). 1,4-Didecyloxybenzene was synthesized from hydroquinone through a Williamson ether route in the presence of a strong base,[28] followed by bromination with bromine in carbon tetrachloride.

The synthesis of the monomers is based on the coupling reaction between alkylzinc chloride and halo-substituted compounds catalyzed by palladium complex.[29] We converted the 3-alkylthiophenes to the corresponding 4-alkyl-2-thienylzinc chlorides by the lithiation of the 3-alkylthiophenes, followed by transmetalation reaction with anhydrous zinc chloride in THF. Since both the 2- and 5-positions of thiophene ring are usually easy to be metalated, to confine the lithiation happening at the 5-position of the thiophene rings, lithium diisopropylamine (LDA), a significantly hindering base, was employed in the synthesis. A 4-alkyl-2-thienylzinc chloride was refluxed with 1,4-dibromobenzene or a substituted 1,4-dibromobenzene in THF in the presence of tetrakis(triphenylphosphine)palladium(0) as catalyst to afford a monomer in high yield, 80−90% after purification.

The ^{1}H and ^{13}C NMR data in the aromatic regions of the monomers **2a**−**f** are summarized in Tables 1 and 2. The assignment of the corresponding protons and carbons is depicted in Scheme 2. The representatives of ^{1}H NMR spectra for **2a** and **2d** and ^{13}C NMR spectra for **2c** and **2f** are displayed in Figures 1 and 2. In the ^{1}H NMR spectra, all of the monomers exhibit three clear

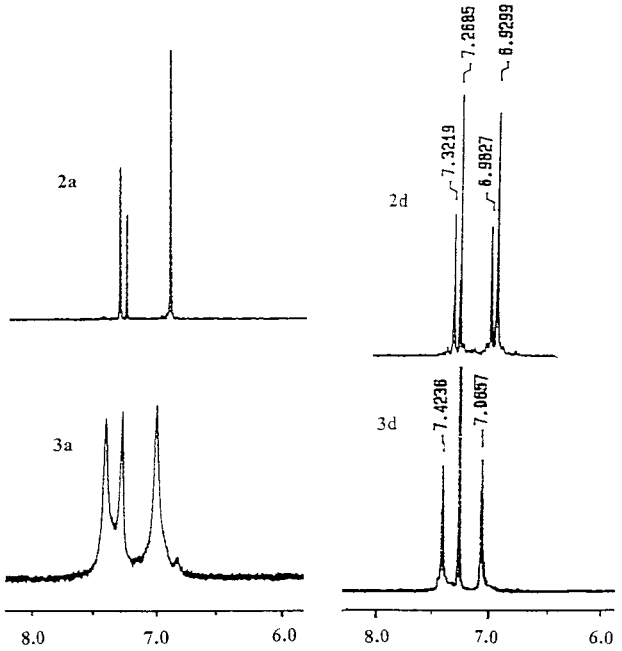

Figure 1. Comparisons of ^{1}H spectra between monomer **2a** and polymer **3a**, and between monomer **2d** and polymer **3d**.

Table 2. ^{13}C NMR Chemical Shifts and Assignment of Monomers 2a−f and Polymers 3a−f

	C-1	C-2	C-3	C-4	C-5	C-6	C-7
2a	143.36	132.04	127.75	142.31	132.38	133.60	119.80
3a	142.34	132.42	128.17	133.32	128.63	133.14	141.50
2b	144.29	125.87	125.87	143.39	124.34	133.48	119.41
3b	143.52	125.91	125.91	133.24	124.66	128.27	143.13
2c	123.12	149.60	111.27	138.71	125.26	125.71	126.60
3c	122.68	149.33	112.10	138.55	126.97	129.30	141.85
2d	149.14	133.06	126.66	142.22	132.48	133.68	118.14
3d	148.69	133.29	128.38	134.21	129.16	133.92	143.47
2e	150.03	125.86	125.86	143.20	123.11	133.53	117.93
3e	149.33	126.03	126.03	133.53	122.80	127.43	143.83
2f	125.61	149.27	112.65	148.78	122.97	138.81	118.73
3f	125.03	149.38	111.94	139.06	122.61	128.16	147.53

Scheme 2. Chemical Structures of the Monomers 2 and Polymers 3 and the Assignments of Protons and Carbons

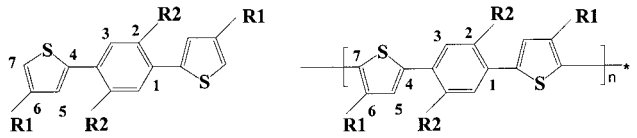

singlet peaks in the aromatic region which correspond to the proton on the phenylene ring and the two separated protons on the thiophene rings. In the ^{13}C NMR spectra, only seven signals in the aromatic region were measured out for each of the monomers. These results prove that we have successfully confined the coupling reaction between the 3-alkylthiophenes and the 1,4-dibromobezenes at the 5-positions of the 3-alkylthiophenes in high selectivity. This can be attributed to the significant steric hindrance of the 3-alkyl groups to the large base of LDA, which results in the high selectivity of lithiation at the 5-positions of the 3-alkylthiophenes. The molecular structural feature of the monomers, in which the alkyl groups are defined at the 4-positions of the thiophene rings, is essential for ensuring structural definition of the resulting polymers in polymerization.

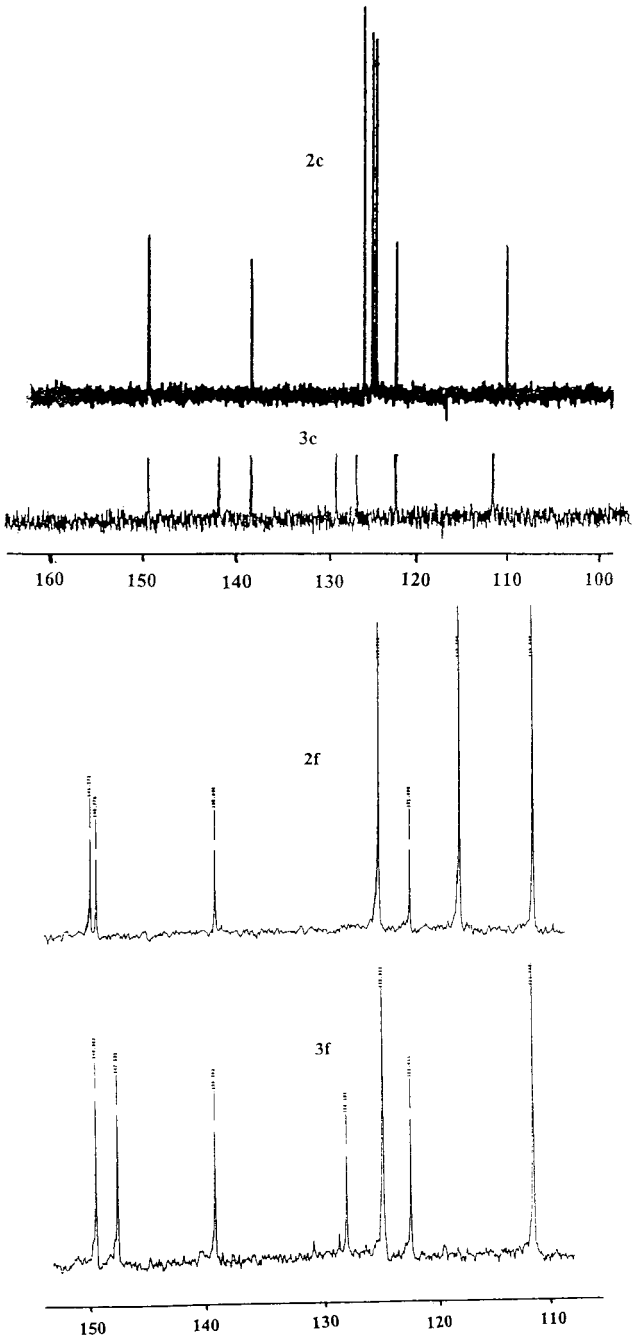

Figure 2. ^{13}C NMR spectra of monomers **2c** and **2f** and polymers **3c** and **3f**.

The polymerization of the monomers was performed through $FeCl_3$ oxidation in chloroform.[30] After being dedoped and purified, the polymers were obtained as yellow powders with the yields around 80%. Elemental analyses showed very good agreement between the experimental and theoretical results for the proposed polymer structures, as described in the Experimental Section. The polymers readily dissolve in common organic solvents, such as THF, chloroform, 1,1,2,2-tetrachloroethane, toluene, and xylene. The number-average molecular weights (M_n) of the polymers were determined by GPC to be 14 000−25 000 with the polydispersibilities of 1.90−2.92 against the polystyrene standards. These results are summarized in Table 3. The polymers were stable up to 300 °C in air as indicated by TGA.

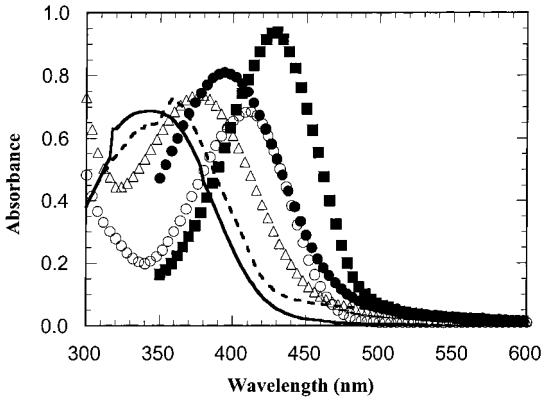

Figure 3. Absorption spectra of polymers **3a** (solid line), **3b** (filled circle), **3c** (filled square), **3d** (dashed line), **3e** (open triangle), and **3f** (open circle).

Table 3. Basic Properties of the Polymers

polym.	polym. color	polym. yield (%)	$M_n \times 10^4$ (g/mol)	polydispersity
3a	light-yellow	83	2.04	2.92
3b	yellow	78	1.97	2.74
3c	yellow	81	1.46	1.92
3d	yellow	73	2.11	2.46
3e	yellow	76	2.31	2.55
3f	yellow	84	1.67	2.01

The ^1H and ^{13}C NMR data of the polymers **3a**−**f** in the aromatic regions are listed in Tables 1 and 2. The ^1H NMR spectra of polymers **3a** and **3d** and the ^{13}C NMR spectra of polymers **3c** and **3f** are compared in Figures 1 and 2, respectively. In the ^1H NMR spectra, all of the polymers contain only two singlets in the aromatic region. Compared with the spectra of the monomers, the signal corresponding to H-7 in each monomer completely disappears after the polymerization. At the same time, the chemical shifts of the other two aromatic protons in the monomers are increased by 0.06−0.20 ppm after the polymerization because of the enhancement of π-delocalization. The results prove that all of the polymers have high regioregularity of head-to-head linkage between two adjacent thiophene rings, similar to those obtained in the polymerization of 4,4′-dialkyl-2,2′-bithiophenes by $FeCl_3$-oxidation, which results in defined HH-TT poly(alkylthiophene)s.[31,32] The complete regiospecificity of the polymers is further supported by the ^{13}C NMR spectra, in which only seven well-resolved resonance signals are observed in the aromatic region for each of the polymers. As illustrated in Scheme 2, the seven signals correspond to the seven aromatic carbons in the polymers. The chemical shifts of C-5 in the monomers are changed from ∼120 to ∼140 ppm after polymerization.

Optical Properties. The films of the polymers were prepared on quartz plates or on microslides by spin-casting the polymers from their solutions in 1,1,2,2-tetrachloroethane (1.5% w/v). The films of polymers **3a** and **3d** are colorless, and the films of other four polymers are yellowish-green. Under ultraviolet light irradiation, the films emit intensive fluorescence with the colors from blue to green. UV−vis absorption spectra and photoluminescence spectra of the polymers were measured from the films and are shown in Figures 3 and 4. The peak wavelengths of the spectra and the $\pi-\pi^*$ band gaps of the polymers estimated from the absorption onset wavelengths are summarized in Table 4. Although all of the six polymers have the same

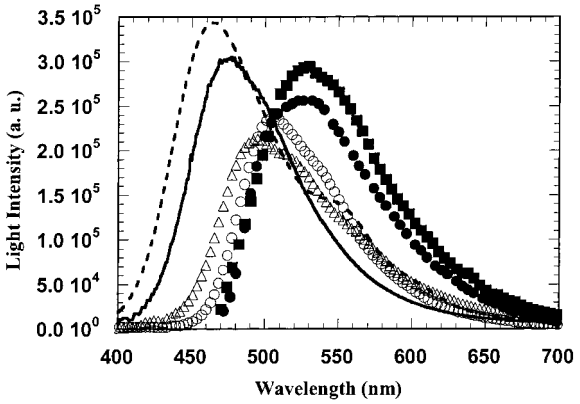

Figure 4. Photoluminescence spectra of polymers **3a** (solid line), **3b** (filled circle), **3c** (filled square), **3d** (dashed line), **3e** (open triangle), and **3f** (open circle).

Table 4. Optical Properties of the Polymers

polym.	abs. λ_{max} (nm)	abs. λ_{onset} (nm)/ band gap (eV)	PL λ_{max} (nm)	Stokes' shift (nm)	PL quantum efficiency (%)
3a	340	470/2.64	477	137	10
3b	396	514/2.41	524	128	20
3c	430	525/2.36	530	100	29
3d	360	455/2.72	466	106	6
3e	376	488/2.54	495	119	11
3f	410	500/2.48	505	95	16

backbone structure, their optical properties are quite different with the variation of substitution. Generally, a substituted group affects the electronic and optical properties of a conjugated polymer in two ways: the electronic structural feature of the substituted group and the steric hindrance arising from the substituted group. These six polymers can be divided into two series in accordance with the substituents on the thiophene ring: a *n*-hexyl-substituted series and a cyclohexyl-substituted series.

For both of the two series, the introduction of two methyl groups into the phenylene ring at the 2- and 5-positions results in a remarkable spectral blue shift. In the *n*-hexyl-substituted series, the blue shifts are 56 nm (396 nm for polymer **3b** → 340 nm for polymer **3a**) in absorption spectra and 47 nm (524 nm for polymer **3b** → 477 nm for polymer **3a**) in photoluminescence spectra. Polymer **3b** is a green light-emitting material, whereas polymer **3a** emits blue light. The same situation happens in the cyclohexyl-substituted series. The emission color of polymer **3e** is bluish-green, and the emission from polymer **3d** is blue. The phenomenon could be understood in terms of the steric effect of the methyl groups on the coplanarity between the phenylene and thiophene rings. Although we do not have the data of the torsional angles between the phenylene and the thiophene rings, it is obvious that the introduction of the methyl groups will increase the torsional angles and thus reduces the effective conjugation in the polymers. On the other hand, the introduction of two decyloxy chains into the 2- and 5-positions of the phenylene ring induces spectral redshift in both of the two series. The absorption spectrum is redshifted by ~35 nm, and the photoluminescence spectrum is redshifted by 6 nm for the *n*-hexyl-substituted series and 10 nm for the cyclohexyl-substituted series. The strong electron-donating property of alkyloxy groups should be responsible for the spectral redshift. The less steric hindrance of alkyloxy groups compared with alkyl substituents should also be considered.[33]

As a bulky substituent, cyclohexyl group may give rise to stronger steric hindrance between two adjacent thiophene rings than *n*-hexyl group does. Replacement of *n*-hexyl group on the thiophene ring with cyclohexyl group may decrease the effective conjugated length in polymers by increasing the torsional angles between thiophene rings and thus results in spectral blue shift in the resulting polymers. This has been demonstrated both experimentally and theoretically in some substituted polythiophenes.[18,34,35] The bulky substituent effect is fully reflected in our new polymers. The $\pi-\pi^*$ band gaps of the cyclohexyl-substituted polymers estimated from absorption onset wavelengths are 0.11 eV (on the average) higher than those of the corresponding *n*-hexyl-substituted polymers. The absorption and photoluminescence spectra of the polymers are blueshifted by 10−30 nm by replacing the *n*-hexyl group with the cyclohexyl group (except the absorption spectrum of polymer **3d** due to unknown reason).

The absolute PL quantum efficiencies of the polymers in neat films were measured in an integrated sphere at room temperature in air following the procedure described by Greenham et al. using an argon ion laser line of 358 nm as the excitation source.[36] The results are listed in Table 4. First, it is noted that the PL quantum efficiencies are significantly higher than those of PTs. For polymer **3c**, η_{PL} was measured to be 29%. This value is higher than that of MEH−PPV (15−18%) and is comparable with that of PPV (~27%).[8] From the consideration of PL quantum efficiency, polymers **3b**, **3c**, and **3f** are valuable for application as EL materials. The results prove that the structural modification of inserting one phenylene ring between every two thiophene rings in polythiophene backbone is a useful approach in increasing the PL quantum efficiency of thiophene-based polymers.

There is pronounced difference in PL quantum efficiencies between the two series of polymers. The polymers in the *n*-hexyl-substituted series exhibit 40−49% higher η_{PL} than that of the corresponding polymers with the same substitution in the cyclohexyl-substituted series. This indicates that the PL process in the polymers may be affected by the substituted groups on the thiophene ring. It is believed that this is associated with the supramolecular organizations in the polymers. The larger nonplanarity of the polymer chain caused by the cyclohexyl-substitution compared to the *n*-hexyl-substitution should make a positive contribution to PL quantum efficiency, according to the assertion demonstrated in poly(alkylthiophene)s.[26] It seems that the "opposite" experimental observation is in connection with the degree of order of the polymer chains in condensed states. It is noted that there is an identifiable vibronic shoulder around 390 nm in the absorption spectrum of polymer **3f** (Figure 3). In contrast, the absorption spectrum of polymer **3c** shows a perfect structureless feature. In the PL spectra (Figure 4), the vibronic shoulders are better resolved for polymers **3d**−**f**, all with the cyclohexyl-substitution on the thiophene ring, whereas the vibronic structure is lacking for polymers **3a**−**c**. A better resolved vibronic structure in conjugated polymers normally corresponds to a higher degree of order of polymer chains. We may thus assume that the cyclohexyl-substituted polymers have higher-degree order of polymer chain in film states than that of the *n*-hexyl-substituted polymers. The assumption of higher-degree order in the cyclohexyl-substituted poly-

mers is also supported by the fact that the Stokes' shifts of the *n*-hexyl-substituted polymers are larger than those of the corresponding cyclohexyl-substituted polymers (Table 4).[26] The optical and structural studies for poly(alkylthiophene)s reveal that the PL quantum efficiency decreases with increasing orientation of the polymer films. For example, head-to-tail regioregular poly(3-alkylthiophene)s have higher orientation than regiorandom poly(3-alkylthiophene)s in films.[37] The PL quantum efficiencies measured from them are 1 and 2% respectively.[26] Poly(4,4′-didecyl-2,2′-bithiophene), a head-to-head and tail-to-tail regioregular poly(alkylthiophene), which has a much lower degree of crystallinity than those of regiorandom poly(3-alkylthiophene)s in films,[38,26] was demonstrated to have a high PL quantum efficiency, 11%.[26] The higher-degree order of polymer chains in the cyclohexyl-substituted polymers may be attributed to the high tendency of crystallization of cyclohexyl ring compared to the *n*-hexyl chain.

On the other hand, the PL quantum efficiency of the polymers is sensitive to the substitution on the phenylene ring for both of the two series. The introduction of methyl groups into the 2- and 5-positions of the phenylene ring cuts off about half of the PL quantum efficiency. The attachment of decyloxy chains into the same positions of the phenylene ring increases the PL quantum efficiency by about 50%. These results cannot be simply interpreted in terms of the steric effects of the substituents or supramolecular organization. There may be some changes of intrinsic electronic properties of the backbone owing to the substitutions.

Electrochemical Properties. The electrochemical properties of all six polymers were investigated in an electrolyte consisting of a 0.10 M tetrabutylammonium hexylfluorophosphate (*n*-Bu_4NPF_6) solution in acetonitrile by cyclic voltammetry. The cyclic voltammograms of the *n*-hexyl-substituted series polymers and the cyclohexyl-substituted series polymers are displayed in Figure 5. Both the oxidative and reductive processes of all of the polymers are reversible. For example, in the anodic scan for polymer **3c**, the oxidation (*p*-doping) process onsets at 0.60 V and gives a sharp oxidation peak at 0.93 V. The rereduction peak appears at 0.75 V. On sweeping the polymer cathodically, the reduction (*n*-doping) begins at −1.82 V. Thereafter the cathodic current increases quickly and produces a cathodic peak at −2.21 V, and a corresponding reoxidation peak occurs at −2.03 V. The clear redox behavior and the good doping reversibility not only prove that the polymers may be good candidates for EL materials for applications in polymer light-emitting diodes and polymer light-emitting electrochemical cells (LECs),[5] but also allow us to characterize and compare the electronic properties of the polymers. The electrochemical data of the polymers obtained from their cyclic voltammograms are summarized in Table 5.The *p*-doping process of the polymers is sensitive to the substitution on the phenylene ring. The attachment of methyl groups at the 2- and 5-positions of the phenylene ring results in an increase of *p*-doping potential. The *p*-doping onset potential of polymer **3a** (0.85 V) is 0.15 V higher than that of polymer **3b** (0.70 V). The increase of oxidative potential arising from the attachment is more clearly evident in the cyclohexyl-substituted series polymers. Compared to polymer **3e**, the *p*-doping onset and peak potentials of polymer **3d** are increased by 0.20 and 0.11 V, respectively. The increase of the oxidation potential

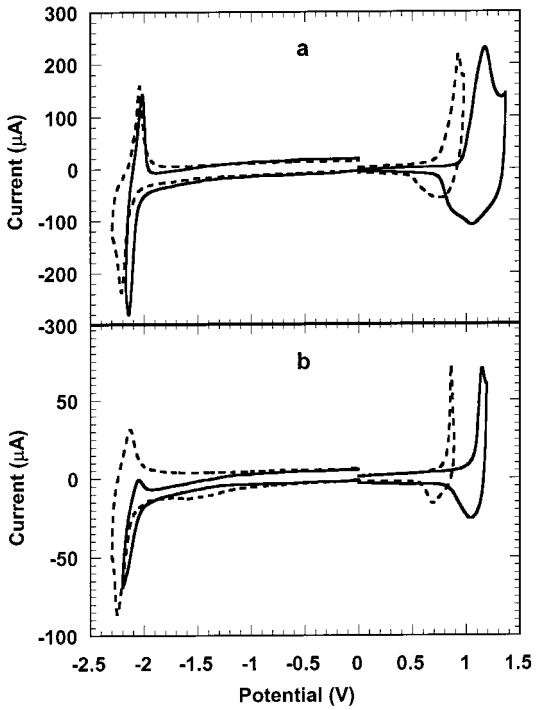

Figure 5. Cyclic voltammograms of polymers **3a** (solid line), **3b** (open circle) and **3c** (dashed line) (a) and polymers **3d** (solid line), **3e** (open circle) and **3f** (dashed line) (b). Measured in 0.10 M *n*-Bu_4NPF_6 in acetonitrile at scan rate of 40 mV/s.

may be attributed to the decrease of effective conjugation of polymer chain resulted from the steric hindrance of the methyl groups. On the contrary, the introduction of decyloxy groups into the 2- and 5-positions of the phenylene ring results in a decrease in oxidation potential. In the *n*-hexyl-substituted series polymers, the peak potential is decreased from 1.28 V in polymer **3b** to 0.93 V in polymer **3c**, and the corresponding onset potential is decreased from 0.70 to 0.60 V. Similarly, in the cyclohexyl-substituted series, the oxidation peak potential is changed from 1.03 V for polymer **3e** to 0.86 V for polymer **3f**, and the onset potential is correspondingly changed from 0.68 to 0.60 V. The decrease of oxidation potential is evident due to the electron-donating feature of decyloxy group, making the polymer more electropositive.

In comparison with the *p*-doping process, the *n*-doping process of the polymers is less sensitive to the variation of substitution at the 2- and 5-positions of the phenylene ring. For the *n*-hexyl-substituted series, polymers **3a**, **3b**, and **3c** onset their *n*-doping processes at −1.80, −1.85, and −1.82 V, respectively, and give rise to their peaks at −2.14, −2.24, and −2.21 V. For the cyclohexyl-substituted polymers, the onset potentials are determined to be −1.90, −1.85, and −1.90 V for polymers **3d**, **3e**, and **3f**, respectively. The *n*-doping peaks occur at −2.30 V for polymer **3e** and at −2.25 V for polymer **3f** (because of the poor peak characterization, the accurate peak potential of polymer **3d** was not obtained).

By comparison between the two series, it is found that the cyclohexyl-substituted polymers have slightly smaller (by 0.03−0.10 V) *p*-doping peak potentials and higher *n*-doping potentials than the corresponding polymers with the same substituted groups on the phenylene ring in the *n*-hexyl-substituted series. This implies that the cyclohexyl-substitution at the 4-position of the thiophene ring makes the resulting polymers more electropositive than the *n*-hexyl-substitution. It is also noted that

Table 5. *p*-Doping and *n*-doping Characteristics of the Polymers

	p-doping (V)[a]			*n*-doping (V)[a]			energy levels (eV)		
polymers	E_{Onset}	E_{pa}	E_{pc}	E_{Onset}	E_{pc}	E_{pa}	HOMO	LUMO	band gap (eV)
3a	0.85	1.17	1.04	−1.80	−2.14	−2.02	−5.24	−2.59	2.65
3b	0.70	1.28	0.90	−1.85	−2.24	−1.93	−5.09	−2.54	2.45
3c	0.60	0.93	0.75	−1.82	−2.21	−2.03	−4.99	−2.57	2.42
3d	0.88	1.14	1.03	−1.90		−2.06		−2.49	
3e	0.68	1.03	0.82	−1.85	−2.30	−2.04	−5.07	−2.54	2.53
3f	0.60	0.86	0.68	−1.90	−2.25	−2.13	−4.99	−2.49	2.50

[a] E_{Onset}, E_{pa}, and E_{pc} stand for onset potential, anodic peak potential, and cathodic peak potential, respectively.

anodically scanned cyclic voltammograms of the cyclohexyl-substituted polymers are remarkably narrower than those of the corresponding *n*-hexyl-substituted polymers with the same substitution on the phenylene ring. Meanwhile, the *n*-hexyl-substituted polymers produce much higher currents both in anodic scans and in cathodic scans than do the cyclohexyl-substituted polymers. The experimental conditions are exactly the same for all of the polymers. Although we did not control the thickness of the polymer films on the electrode, we believe that they are comparable because the films were prepared under the same environmental conditions and all of the polymer solutions had the same concentration. We may conclude from the phenomenon that the *n*-hexyl-substituted polymers have higher doping degrees than those of the cyclohexyl-substituted polymers.[39] The higher doping degrees of *n*-hexyl-substituted polymers may be associated with the better coplanarity between conjugated rings and less crystallization tendency of the polymer in this series, as discussed above.

The onset potentials of *p*- (ϕ_p') and *n*-doping (ϕ_n') are used to determine the HOMO and LUMO energy levels of the conjugated polymers using the empirical relationship proposed by Leeuw et al.[40] In this work, $E_{LUMO} = -(\phi_n' + 4.39)$ (eV), and $E_{HOMO} = -(\phi_p' + 4.39)$ (eV), where E_{LUMO} is the LUMO energy level and E_{HOMO} is the HOMO energy level below the vacuum. The calculated results are listed in Table 5. The data are useful for the selection of electrode materials and charge-transporting materials in the fabrication of polymer LEDs. The difference of the *p*-doping onset potential and the *n*-doping potential of a conjugated polymer may be used to estimate the energy gap of the polymer. The electrochemical energy gaps, $\Delta\phi$ ($=\phi_p' - \phi_n'$), of the polymers are also summarized in Table 5, which are close to the optically determined ones.

To investigate the electrochemical stability of the polymers, multiscans were performed on polymer films. The results demonstrated good electrochemical stability of the polymers. One representative of multiscan cyclic voltammograms is displayed in Figure 6. After 10 cyclic scans, both the doping potentials and the currents are almost maintained unchanged. After the 20th scan, only a light change can be observed in the cyclic voltammograms.

Light-Emitting Diodes from the Polymers. Polymers **3a**−**c** and **3f**, whose PL quantum yields are above 10%, were chosen to fabricate polymer light-emitting diodes with the configuration of ITO/polymer/Al or Ca to demonstrate the electroluminescence of the new polymers.

Under the forward bias (ITO wired as positive), all of the diodes emitted visible lights above sufficient voltages. The electroluminescence from polymer **3a** is blue, the emission from polymer **3f** is bluish green, and the other two polymers emit green light in the devices. The

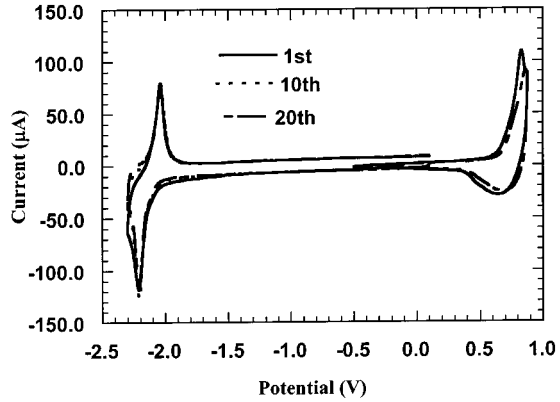

Figure 6. Cyclic voltammograms for polymer **3c** showing the first, 10th and 20th cycles in 0.10 M *n*-Bu_4NPF_6 in acetonitrile. Scan rate: 40 mV/s. Room temperature.

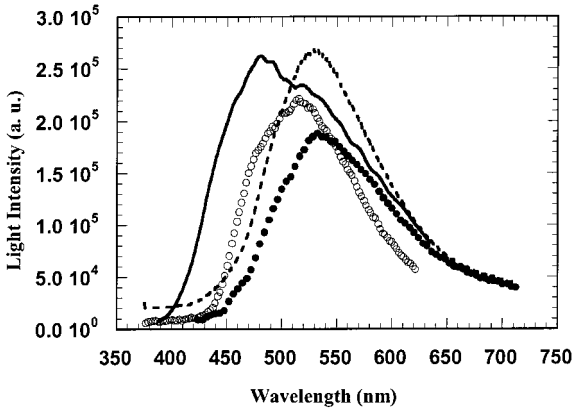

Figure 7. Electroluminescent spectra of polymers **3a** (solid line), **3b** (filled circle), **3c** (dashed line) and **3f** (open circle). Measured from the devices with the configuration of ITO/polymer/Ca.

Table 6. Turn-On Voltages and EL External Efficiencies of Light-Emitting Diodes Based on Polymers

devices based on polymers	turn-on voltages (V) cathode materials		EL external efficiencies (%) cathode materials	
	Ca	Al	Ca	Al
3a	17	17	0.004	0.0001
3b	13	15	0.02	0.005
3c	8	9	0.1	0.05
3f	9	10	0.05	0.008

electroluminescence spectra of the four polymers are shown in Figure 7. For the same polymers, the EL spectra recorded from the devices using Al and Ca as cathodes are identical. However, the EL performance of the polymers is significantly different from each other. The device characteristics of the polymers are summarized in Table 6, and the curves of current and light output versus bias voltage of the device ITO/polymer **3c**/Ca are given in Figure 8 as a representative. For polymer **3a**, the turn-on voltages are very high (∼17 V)

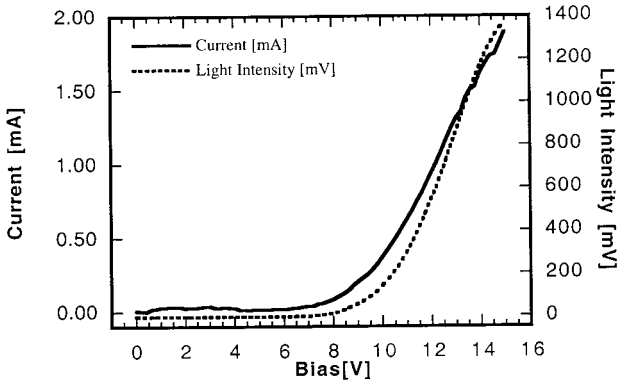

Figure 8. Current and light intensity vs. bias voltage in ITO/polymer **3c**/Ca device.

either using Al or using Ca as the cathode. The turn-on voltage decreases remarkably on going from polymer **3a** to polymer **3c**. The devices of polymer **3c** turn-on around 8 V. At the same time, the external EL quantum efficiencies measured from polymer **3b** are about 1 order higher in magnitude than those measured from polymer **3a**. From polymer **3b** to polymer **3c**, another 1 order of magnitude improvement in external EL quantum efficiency was observed, and a relatively high external EL quantum efficiency of 0.1% was achieved by using Ca cathode. The fact that changing the cathode material from Al to Ca does not decrease the turn-on voltage significantly indicates that the turn-on voltages of the devices are dominated by hole-injection at the anode contacts. Referring to the data of HOMO and LUMO levels of the polymers in Table 5, we may attribute the decrease of turn-on voltage and the improvement of EL quantum efficiency from polymer **3a** to polymer **3c** to the increase of HOMO energy level, from −5.24 eV in polymer **3a** to −4.99 eV in polymer **3c**. The increase of HOMO energy level lowers the energy barrier for the hole-injection from ITO (bearing a work function of 4.7 eV) electrode to the polymer layer and thus results in the decrease of driving voltage and the improvement of quantum efficiency. Polymer **3f** has a very similar HOMO energy level with polymer **3c**, so the devices fabricated from the two polymers exhibit very close turn-on voltages. The lower EL quantum efficiencies of polymer **3f** compared with polymer **3c** may be attributed to the higher LUMO level in polymer **3f**, which makes a higher energy barrier for electron injection at cathode contact. Similar considerations can explain the improvement of external EL quantum efficiency by changing the cathode material from Al (with the work function of 4.3 eV) to Ca (with the work function of 2.9 eV) for each of the polymers.[41] In each case of the devices presented here, the energy barriers both for hole injection and for electron injection are high. Therefore, better EL performance from the polymers can be expected by adding suitable charge-injecting and charge-transporting layers to facilitate the charge injections and balance the currents between electrons and holes.

Conclusions

A new series of soluble thiophene-based conjugated polymers have been synthesized as light-emitting materials through $FeCl_3$-oxidative polymerization, a facile and popular method in the preparation of polythiophene derivatives. Because of the successful selective control of lithiation at the 5-position of 3-substituted thiophene ring for the preparation of monomers by using a high hindrance base, the resulting polymers have high regioregularity with perfect head-to-head linkage between two adjacent thiophene rings. Some important advantages of substituted polythiophenes, such as facility of synthesis, good solubility, good thermal, and electrochemical stability, have been demonstrated to be maintained in the new polymers, while the PL quantum efficiency is dramatically increased compared with those of conventional polythiophene materials. The demonstrated high absolute PL quantum efficiencies (up to 29%) of the polymers in neat films reveal the value for their applications as EL materials in polymer light-emitting diodes. We may conclude that inserting suitable substituted phenylene rings into the backbone of polythiophene is an efficient structural modification approach for improving the PL efficiency of thiophene-based conjugated polymers. The optical and electronic properties of the polymers may be tuned by attaching different functional groups on different positions of the backbone. Blue to green light emission was demonstrated with the backbone structure. Because it was found that the substitutions on both the phenylene ring and the thiophene ring remarkably affect the PL quantum efficiency of the resulting polymers, we believe that there is still some niches to further improve the PL quantum efficiency of the series of polymers by carefully selecting substituents. The relatively high EL performance of the polymers in simple single-layered devices and the potential of further improvement in EL performance by improving charge injections demonstrate that the polymers are good candidates of emissive materials for polymer light-emitting diodes.

References and Notes

(1) (a) Burroughes, J. H.; Bradley, D. D. C.; Brown, A. R.; Marks, R. N.; Mackay, K.; Friend, R. H.; Burns, P. L.; Holmes, A. B. *Nature* **1990**, *347*, 539. (b) Gustafsson, G.; Cao, Y.; Treacy, G. M.; Klavetter, F.; Colaneri, N.; Heeger, A. J. *Nature* **1992**, *357*, 477.
(2) (a) Yu, G.; Gao, J.; Hummelen, J. C.; Wudl, F.; Heeger, A. J. *Science* **1995**, *270*, 1789. (b) Halls, J. J. M.; Walsh, C. A.; Marseglia, E. A.; Frienf, R. H.; Moratti, S. C.; Holmes, A. B. *Nature* **1995**, *376*, 498.
(3) Burroughes, J. H.; Jones, C. A; Friend, R. H. *Nature* **1988**, *335*, 137.
(4) Yang, Y.; Heeger, A. J. *Nature* **1994**, *372*, 344.
(5) (a) Pei, Q.; Yu, G.; Zhang, C.; Yang, Y.; Heeger, A. J. *Science* **1995**, *269*, 1086. (b) Pei, Q.; Yu, G.; Zhang, C.; Heeger, A. J. *J. Am. Chem. Soc.* **1996**, *118*, 3922.
(6) Hide, H.; Díaz-García, M. A.; Schwartz, B. J.; Andersson, M. R.; Pei, Q.; Heeger, A. J. *Science* **1996**, *273*, 1833.
(7) Kraft, A.; Grimsdale, A. C.; Holmes, A. B. *Angew. Chem. Int. Ed.* **1997**, *37*, 4402.
(8) Friend, R. H.; Gymer, R. W.; Holmes, A. B.; Buuroughes, J. H.; Marks, R. N.; Taliani, C.; Bradley, D. D. C.; Dos Santos, D. A.; Brédas, J. L.; Lögdlund, M.; Salaneck, W. R. *Nature* **1999**, *397*, 121.
(9) Heeger, A. J. *Solid State Commun.* **1998**, *107*, 673.
(10) Tourillon, G. *Handbook of Conducting Polymers*; Skotheim, T. J., Ed.; Marcel Dekker: New York, 1986; Vol. 1, p 293.
(11) (a) Roncali, J. *Chem. Rev.* **1992**, *92*, 711. (b) Roncali, J. *Chem. Rev.* **1997**, *97*, 173.
(12) McCullough, R. D. *Adv. Mater.* **1998**, *10*, 93.
(13) Berggren, M.; Inganäs, O.; Gustafsson, G.; Rasmusson, J.; Andersson, M. R.; Hjertberg, T.; Wennerström, O. *Nature* **1994**, *372*, 444.
(14) Andersson, M. R.; Berggren, M.; Inganäs, O.; Gustafsson, G.; Gustafsson-Carlberg, J. C.; Selse, D.; Hjertberg, T.; Wennerström, O. *Macromolecules* **1995**, *28*, 7525.
(15) Bradley, D. D. C. *Synth. Met.* **1993**, *54*, 401.
(16) Inganäs, O.; Granlund, T.; Theander, M.; Berggren, M.; Andersson, M. R.; Ruseckas, A.; Sundström, V. *Opt. Mater.* **1998**, *9*, 104.
(17) Beljonne, D.; Cornil, J.; Friend, R. H.; Janssen, R. A. J.; Bredas, J. L. *J. Am. Chem. Soc.* **1996**, *118*, 6453.

(18) Berggren, M.; Gustafsson, G.; Inganäs, O.; Andersson, M. R.; Wennerström, O.; Hjerberg, T. *Adv. Mater.* **1994,** *6*, 488.
(19) Granlund, T.; Theander, M.; Berggren, M.; Andersson, M.; Ruzeckas, A.; Sundström, V.; Björk, G.; Granström, M.; Inganäs, O. *Chem. Phys. Lett.* **1998**, *288*, 879.
(20) Andersson, M.; Yu, G.; Heeger, A. J. *Synth. Met.* **1997**, *85*, 1275.
(21) Yang, Y.; Pei, Q.; Heeger, A. J. *J. Appl. Phys.* **1996**, *79*, 934.
(22) Pei, Q.; Yang, Y. J. *Am. Chem. Soc.* **1996**, *118*, 7416.
(23) Grice, A. W.; Bradley, D. D. C.; Bernius, M. T.; Inbasekaran, M.; Wu, W. W.; Woo, E. P. *Appl. Phys. Lett.* **1998**, *73*, 629.
(24) Gigli, G.; Barbarella, G.; Favaretto, L.; Cacialli, F.; Cingolani, R. *Appl. Phys. Lett.* **1999**, *75*, 439.
(25) Reynolds, J. H.; Ruiz, J. P.; Child, A. D.; Nayak, K.; Marynick, D. S. *Macromolecules* **1991**, *24*, 678. (b) Ruiz, J. P.; Dharia, J. R.; Reynolds, J. R. *Macromolecules* **1992,** *25*, 849.
(26) Barta, P.; Cacialli, F.; Friend, R. H.; Zagórska, M. *J. Appl. Phys.* **1998**, *84*, 6279.
(27) McCullough, R. D.; Lowe, R. D.; Jayaraman, M.; Anderson, D. L. *J. Org. Chem.* **1993**, *58*, 904.
(28) Gallent, J. B. *J. Org. Chem.* **1958**, *23*, 75.
(29) Pelter, A.; Maud, J. M.; Jenkins, I.; Sadeka, C.; Coles, G. *Tetrahedron Lett.* **1988**, *9*, 743.
(30) Leclerc, M.; Diaz, F. M.; Wegner, G. *Makromol. Chem.* **1989**, *190*, 3105.
(31) Zagorska, M.; Kulszewicz-Bajer, I.; Pron, A.; Firlcj, L.; Berier, P.; Galtier, M. *Synth. Met.* **1991**, *45*, 385.
(32) Zagorska, M.; Krishe, B. *Polymer* **1990**, *31*, 1379.
(33) Meille, S. V.; Farina, A.; Bezziccheri, F.; Gallazzi, M. C. *Adv. Mater.* **1994**, *6*, 848.
(34) Goedel, W. A.; Somanathan, N. S.; Enkelmann, V.; Wegner, G. *Makromol. Chem.* **1992**, *193*, 1195.
(35) Themans, B.; Salaneck, W. R.; Bredas, J. L. *Synth. Met.* **1989**, *28*, C359.
(36) Greenham, N. C.; Samuel, I. D. W.; Hayes, G. R.; Philips, R. T.; Kessener, Y. A. R. R.; Moratti, S. C.; Holmes, A. B.; Friend, R. H. *Chem. Phys. Lett.* **1995**, *241*, 89.
(37) McCullough, R. D.; Williams, S. P.; Tristram-Nagle, S.; Jayaraman, M.; Ewbank, P. C.; Miller, L. *Synth. Met.* **1995**, *69*, 279.
(38) Luzny, W.; Pron, A. *Synth. Met.* **1997**, *84*, 573.
(39) Li, Y.-F.; Cao, Y.; Gao, J.; Wang, D.-L.; Yu, G.; Heeger, A. J. *Synth. Met.* **1999**, *99*, 243.
(40) Leeuw, D. M.; Simenon, M. M. J.; Brown, A. R.; Einerhand, R. E. F.*; Synth. Met.* **1997**, *87*, 53.
(41) Parker, I. D. *J. Appl. Phys.* **1994**, *75*, 1656.

MA9914220